# Hyperspectral Image Denoising via Convex Low-Fibered-Rank Regularization

**Yu-Bang Zheng**

Ting-Zhu Huang, Xi-Le Zhao, Tai-Xiang Jiang, and Jie Huang

University of Electronic Science and Technology of China (UESTC)

30 July 2019

## Outline

1. Introduction
2. The Proposed Model and Algorithm
3. Numerical Experiments

## Hyperspectral Image (HSI)

HSIs contain wealthy spatial-spectral knowledge and have been widely used in many applications, such as material identification, mineral detection, and forest inspection.

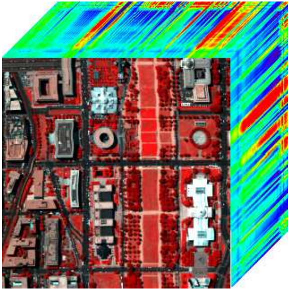

## Why Study HSI Denoising?

HSIs in real applications always suffer from various noises, such as Gaussian noise, sparse noise, and stripes.

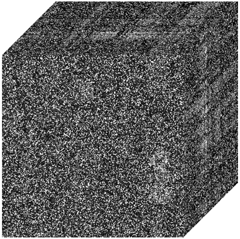

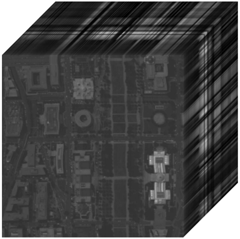

## Conclusive Issue for HSI Denoising

Exploring accurate spatial-spectral prior knowledge of HSIs:

- piecewise smoothness;
- nonlocal self-similarity;
- low rankness;
- $\cdots$

## Tensor

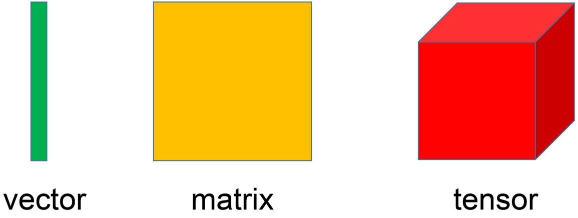

## Tensor Basics (Fibers and Slices)

A *fiber* of a tensor $\mathcal{X}$ is a vector generated by fixing every index but one.

A *slice* of a tensor $\mathcal{X}$ is a matrix generated by fixing every index but two.

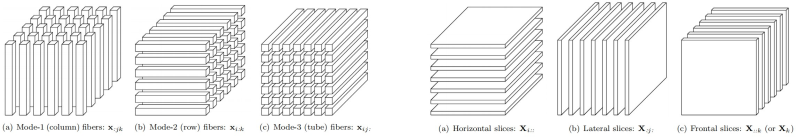


(a) (b)

Figure 1: Fibers and slices of three-way tensors.

## T-Product, T-SVD, and Tubal Rank

M-product: $F = X \cdot Y \quad \Leftrightarrow \quad F(i,j) = \sum_{t=1}^{n_2} X(i,t)Y(t,j).$

T-product: $\mathcal{F} = \mathcal{X} * \mathcal{Y} \Leftrightarrow \mathcal{F}(i,j,:) = \sum_{t=1}^{n_2} \mathcal{X}(i,t,:) \star \mathcal{Y}(t,j,:),$
where $\star$ denotes the circular convolution between two tubes.

## T-Product, T-SVD, and Tubal Rank

M-product: $F = X \cdot Y \;\; \Leftrightarrow \;\; F(i,j) = \sum_{t=1}^{n_2} X(i,t)Y(t,j)$.

T-product: $\mathcal{F} = \mathcal{X} * \mathcal{Y} \Leftrightarrow \mathcal{F}(i,j,:) = \sum_{t=1}^{n_2} \mathcal{X}(i,t,:) \star \mathcal{Y}(t,j,:)$, where $\star$ denotes the circular convolution between two tubes.

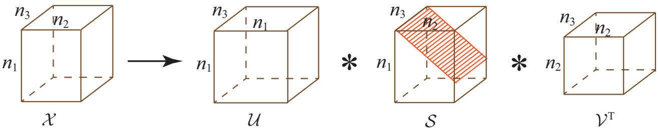


Figure 2: The t-SVD for three-way tensors.

## T-Product, T-SVD, and Tubal Rank

M-product: $F = X \cdot Y \quad \Leftrightarrow \quad F(i,j) = \sum_{t=1}^{n_2} X(i,t)Y(t,j).$

T-product: $\mathcal{F} = \mathcal{X} * \mathcal{Y} \Leftrightarrow \mathcal{F}(i,j,:) = \sum_{t=1}^{n_2} \mathcal{X}(i,t,:) \star \mathcal{Y}(t,j,:),$
where $\star$ denotes the circular convolution between two tubes.

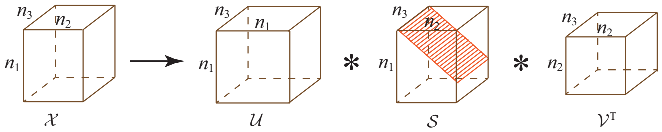


Figure 2: The t-SVD for three-way tensors.

The tubal rank of $\mathcal{X}$ is defined as the number of non-zero tubes of $\mathcal{S}$, i.e., $\mathrm{rank_t}(\mathcal{X}) := \#\{i : \mathcal{S}(i,i,:) \neq 0\}$.

## Motivation

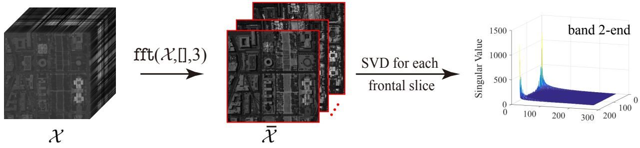


Figure 3: The t-SVD for an HSI.

When setting the band of an HSI to be the frontal slice of a three-way tensor, the t-SVD characterizes its spatial correlations via SVDs, while describes its spectral correlation by the embedded circular convolution or DFT.

## The Proposed Mode-$k$ T-Product

Mode-$k$ t-product ($*_k$):

$$\mathcal{F} = \mathcal{X} *_1 \mathcal{Y} \Leftrightarrow \mathcal{F}(:, j, s) = \sum_{t=1}^{n_3} \mathcal{X}(:, j, t) \star \mathcal{Y}(:, t, s),$$

$$\mathcal{F} = \mathcal{X} *_2 \mathcal{Y} \Leftrightarrow \mathcal{F}(i, :, s) = \sum_{t=1}^{n_1} \mathcal{X}(t, :, s) \star \mathcal{Y}(i, :, t),$$

$$\mathcal{F} = \mathcal{X} *_3 \mathcal{Y} \Leftrightarrow \mathcal{F}(i, j, :) = \sum_{t=1}^{n_2} \mathcal{X}(i, t, :) \star \mathcal{Y}(t, j, :).$$

## The Proposed Mode-*k* T-SVD and Fibered Rank

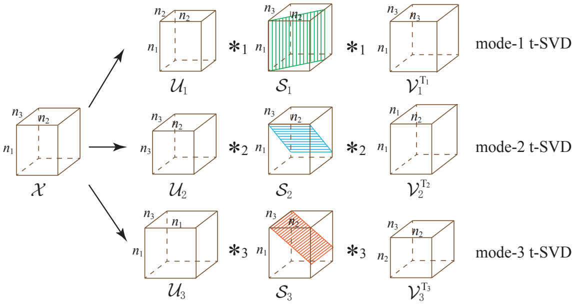


Figure 4: The mode-*k* t-SVD for three-way tensors (*k*=1,2,3).

## The Proposed Mode-$k$ T-SVD and Fibered Rank

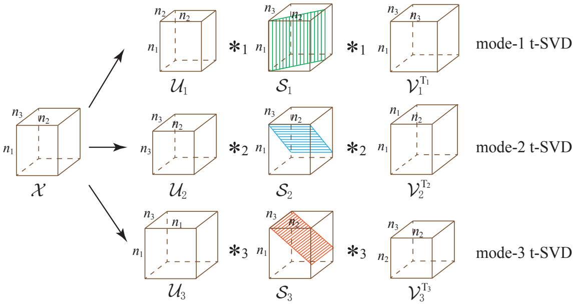


Figure 4: The mode-$k$ t-SVD for three-way tensors ($k$=1,2,3).

The mode-$k$ fibered rank: $\mathrm{rank}_{\mathrm{f}_k}(\mathcal{X})$ is defined as the number of non-zero mode-$k$ fibers of $\mathcal{S}_k$.

## The Proposed Mode-*k* T-SVD and Fibered Rank

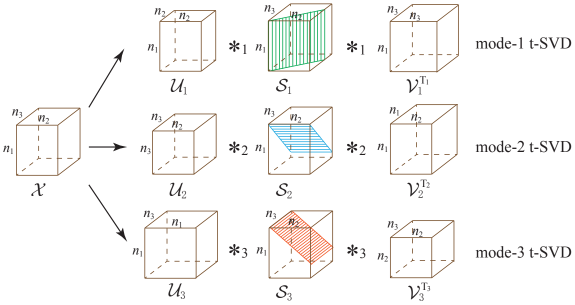


Figure 4: The mode-*k* t-SVD for three-way tensors (*k*=1,2,3).

The mode-*k* fibered rank: $\mathrm{rank}_{f_k}(\mathcal{X})$ is defined as the number of non-zero mode-*k* fibers of $\mathcal{S}_k$.

The fibered rank: $\mathrm{rank}_f(\mathcal{X}) = \left(\mathrm{rank}_{f_1}(\mathcal{X}), \mathrm{rank}_{f_2}(\mathcal{X}), \mathrm{rank}_{f_3}(\mathcal{X})\right)$.

## Low-Fibered-Rank Prior for An HSI

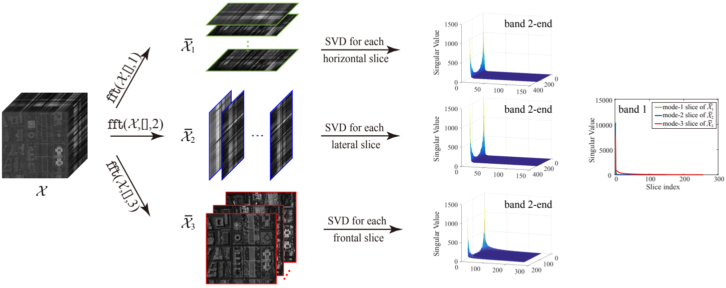


Figure 5: The mode-$k$ t-SVD for an HSI.

## Low-Fibered-Rank Prior for An HSI

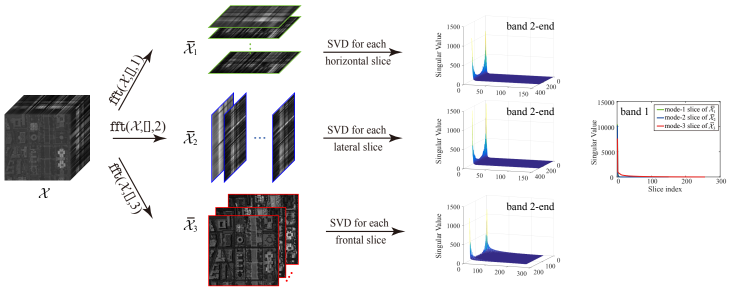


Figure 5: The mode-$k$ t-SVD for an HSI.

Table 1: The rank estimation of an HSI.

| Data | Size | Tucker rank | Tubal rank | Fibered rank |
|---|---|---|---|---|
| *Washington DC Mall* | $256 \times 256 \times 150$ | (107,110,6) | 182 | (8,8,182) |

## Convex Relaxation: Three-Directional Tensor Nuclear Norm (3DTNN)

Mode-$k$ TNN: $\|\mathcal{X}\|_{\text{TNN}_k}$ is defined as the sum of singular values of all the mode-$k$ slices of $\bar{\mathcal{X}}_k$, i.e.,

$$\|\mathcal{X}\|_{\text{TNN}_k} := \sum_{i=1}^{n_k} \|(\bar{X}_k)_k^{(i)}\|_*,$$

where $(\bar{X}_k)_k^{(i)}$ is the $i$-th mode-$k$ slice of $\bar{\mathcal{X}}_k$ with $\bar{\mathcal{X}}_k = \texttt{fft}(\mathcal{X}, [], k)$.

## Convex Relaxation: Three-Directional Tensor Nuclear Norm (3DTNN)

Mode-$k$ TNN: $\|\mathcal{X}\|_{\text{TNN}_k}$ is defined as the sum of singular values of all the mode-$k$ slices of $\bar{\mathcal{X}}_k$, i.e.,

$$\|\mathcal{X}\|_{\text{TNN}_k} := \sum_{i=1}^{n_k} \|(\bar{X}_k)_k^{(i)}\|_*,$$

where $(\bar{X}_k)_k^{(i)}$ is the $i$-th mode-$k$ slice of $\bar{\mathcal{X}}_k$ with $\bar{\mathcal{X}}_k = \texttt{fft}(\mathcal{X}, [], k)$.

3DTNN: $\|\mathcal{X}\|_{\text{3DTNN}}$ is defined as

$$\|\mathcal{X}\|_{\text{3DTNN}} := \sum_{k=1}^{3} \alpha_k \|\mathcal{X}\|_{\text{TNN}_k},$$

where $\alpha_k \geq 0$ $(k = 1, 2, 3)$ and $\sum_{k=1}^{3} \alpha_k = 1$.

## Outline

1. Introduction
2. The Proposed Model and Algorithm
3. Numerical Experiments

## 3DTNN-Based HSI Denoising Model

Considering a target HSI $\mathcal{X} \in \mathbb{R}^{n_1 \times n_2 \times n_3}$, the proposed 3DTNN-based HSI denoising model is formulated as

$$\begin{aligned} \min_{\mathcal{X},\mathcal{N},\mathcal{S}} \ & \|\mathcal{X}\|_{\text{3DTNN}} + \lambda_1 \|\mathcal{N}\|_F^2 + \lambda_2 \|\mathcal{S}\|_1, \\ \text{s.t.} \ & \mathcal{Y} = \mathcal{X} + \mathcal{N} + \mathcal{S}, \end{aligned} \tag{1}$$

where $\mathcal{Y}$ is the observed HSI, $\mathcal{N}$ is Gaussian noise, and $\mathcal{S}$ is sparse noise.

## 3DTNN-Based HSI Denoising Model

Considering a target HSI $\mathcal{X} \in \mathbb{R}^{n_1 \times n_2 \times n_3}$, the proposed 3DTNN-based HSI denoising model is formulated as

$$\begin{aligned} \min_{\mathcal{X},\mathcal{N},\mathcal{S}} \; & \|\mathcal{X}\|_{\text{3DTNN}} + \lambda_1 \|\mathcal{N}\|_F^2 + \lambda_2 \|\mathcal{S}\|_1, \\ \text{s.t.} \;\; & \mathcal{Y} = \mathcal{X} + \mathcal{N} + \mathcal{S}, \end{aligned} \tag{1}$$

where $\mathcal{Y}$ is the observed HSI, $\mathcal{N}$ is Gaussian noise, and $\mathcal{S}$ is sparse noise. The problem (1) can be rewritten as

$$\begin{aligned} \min_{\mathcal{X},\mathcal{N},\mathcal{S}} \; & \sum_{k=1}^{3} \alpha_k \|\mathcal{X}\|_{\text{TNN}_k} + \lambda_1 \|\mathcal{N}\|_F^2 + \lambda_2 \|\mathcal{S}\|_1, \\ \text{s.t.} \;\; & \mathcal{Y} = \mathcal{X} + \mathcal{N} + \mathcal{S}, \end{aligned} \tag{2}$$

## ADMM-Based Algorithm

We use the ADMM to solve (2). We introduce three auxiliary tensors $\mathcal{Z}_k$ ($k = 1, 2, 3$) and reformulate (2) as

## ADMM-Based Algorithm

We use the ADMM to solve (2). We introduce three auxiliary tensors $\mathcal{Z}_k$ $(k = 1, 2, 3)$ and reformulate (2) as

$$\begin{aligned} \min_{\mathcal{X},\mathcal{N},\mathcal{S},\mathcal{Z}_k} \ & \sum\nolimits_{k=1}^{3} \alpha_k \|\mathcal{Z}_k\|_{\mathrm{TNN}_k} + \lambda_1 \|\mathcal{N}\|_F^2 + \lambda_2 \|\mathcal{S}\|_1, \\ \text{s.t. } \ & \mathcal{Y} - (\mathcal{X} + \mathcal{N} + \mathcal{S}) = 0, \ \ \mathcal{X} - \mathcal{Z}_k = 0, \ k = 1, 2, 3. \end{aligned} \tag{3}$$

## ADMM-Based Algorithm

We use the ADMM to solve (2). We introduce three auxiliary tensors $\mathcal{Z}_k$ $(k = 1, 2, 3)$ and reformulate (2) as

$$\min_{\mathcal{X},\mathcal{N},\mathcal{S},\mathcal{Z}_k} \sum_{k=1}^{3} \alpha_k \|\mathcal{Z}_k\|_{\text{TNN}_k} + \lambda_1 \|\mathcal{N}\|_F^2 + \lambda_2 \|\mathcal{S}\|_1, \quad \text{s.t. } \mathcal{Y} - (\mathcal{X} + \mathcal{N} + \mathcal{S}) = 0, \ \mathcal{X} - \mathcal{Z}_k = 0, \ k = 1, 2, 3. \tag{3}$$

The augmented Lagrangian function of (3) is

$$L_{\mu_k,\beta}(\mathcal{Z}_k, \mathcal{X}, \mathcal{N}, \mathcal{S}, \mathcal{M}_k, \mathcal{P}) = \sum_{k=1}^{3} \Big\{\alpha_k \big\|\mathcal{Z}_k\big\|_{\text{TNN}_k} + \langle \mathcal{X} - \mathcal{Z}_k, \mathcal{M}_k\rangle + \mu_k/2 \big\|\mathcal{X} - \mathcal{Z}_k\big\|_F^2 \Big\} + \lambda_1 \|\mathcal{N}\|_F^2 + \lambda_2 \|\mathcal{S}\|_1 + \langle \mathcal{Y} - (\mathcal{X} + \mathcal{N} + \mathcal{S}), \mathcal{P}\rangle + \beta/2 \big\|\mathcal{Y} - (\mathcal{X} + \mathcal{N} + \mathcal{S})\big\|_F^2.$$

## ADMM-Based Algorithm

**Algorithm 1** ADMM-based optimization algorithm for the 3DTNN-based HSI denosing model.

**Input:** The noisy HSI $\mathcal{Y}$, parameters $\alpha = (\alpha_1, \alpha_2, \alpha_3)$, $\mu = (\mu_1, \mu_2, \mu_3)$, $\lambda_1$, $\lambda_2$, $\beta$ and $\rho = 1.2$.

**Initialization:** $p = 0$, $\mathcal{X}^0 = 0$, $\mathcal{N}^0 = 0$, $\mathcal{S}^0 = 0$, $\mathcal{Z}_k^0 = 0$, $\mathcal{M}_k^0 = 0$, and $\mathcal{P}^0 = 0$.

**while** not converged **do**

Update $\mathcal{Z}_k^{p+1} = \mathcal{D}_{\alpha_k/\mu_k}(\mathcal{X}^p + \mathcal{M}_k^p/\mu_k, k)$, $k = 1, 2, 3$.

Update $\mathcal{X}^{p+1} = \left(\sum_{k=1}^3(\mu_k \mathcal{Z}_k^{p+1} - \mathcal{M}_k^p) + (\beta\mathcal{Y} - \beta\mathcal{N}^p - \beta\mathcal{S}^p + \mathcal{P}^p)\right)/(\sum_{k=1}^3 \mu_k + \beta)$.

Update $\mathcal{N}^{p+1} = (\beta\mathcal{Y} - \beta\mathcal{X}^{p+1} - \beta\mathcal{S}^p + \mathcal{P}^p)/(2\lambda_1 + \beta)$.

Update $\mathcal{S}^{p+1} = \mathrm{shrink}(\mathcal{Y} - \mathcal{X}^{p+1} - \mathcal{N}^{p+1} + \frac{\mathcal{P}^p}{\beta}, \frac{\lambda_2}{\beta})$.

Update $\mathcal{M}_k^{p+1} = \mathcal{M}_k^p + \mu_k(\mathcal{X}^{p+1} - \mathcal{Z}_k^{p+1})$, $k = 1, 2, 3$; $\mathcal{P}^{p+1} = \mathcal{P}^p + \beta(\mathcal{Y} - (\mathcal{X}_k^{p+1} + \mathcal{N}_k^{p+1} + \mathcal{S}_k^{p+1}))$.

Let $\mu = \rho\mu$; $\beta = \rho\beta$; $p = p + 1$.

Check the convergence condition $\|\mathcal{X}^{(p+1)} - \mathcal{X}^{(p)}\|_F / \|\mathcal{X}^{(p)}\|_F < 10^{-4}$.

**end while**

**Output:** The restored HSI $\mathcal{X}$.

## Computational Cost and Convergence

Computational cost:

$$\mathcal{O}\Big(n_1 n_2 n_3 \big( \log(n_1 n_2 n_3) + \sum_{i=1}^{3} \min(n_i, n_{i+1})\big)\Big), \text{ where } n_4 = n_1.$$

## Computational Cost and Convergence

Computational cost:

$$\mathcal{O}\Big(n_1 n_2 n_3 \big(\log(n_1 n_2 n_3) + \sum_{i=1}^{3} \min(n_i, n_{i+1})\big)\Big), \text{ where } n_4 = n_1.$$

Convergence:

guaranteed theoretically $\Leftarrow$ convex optimization problem

## Outline

1 Introduction

2 The Proposed Model and Algorithm

3 Numerical Experiments

## Compared Methods

Compared Methods:

- BM4D+TRPCA [*Maggioni et al., IEEE TIP 2012; Lu et al., CVPR 2016*];
- SSTV [*Aggarwal and Majumdar, IEEE GRSL 2016*];
- LRMR [*Zhang et al., IEEE TGRS 2016*];
- LRTR [*Fan et al., IEEE JSTARS 2017*].

## Case 1: different Gaussian noise, fixed impulse noise, and fixed stripe noise.

Table 2: The performance comparison of five competing methods with respect to different Gaussian noise levels.

| Case | Case 1 | | | | | | | | |
|---|---|---|---|---|---|---|---|---|---|
| Gaussian noise | $\sigma = 0.02$ | | | $\sigma = 0.06$ | | | $\sigma = 0.10$ | | |
| Impulse noise | proportion $\upsilon = 0.2$ | | | | | | | | |
| Stripes | added to 10 bands and proportion $p = 10\%$. | | | | | | | | |
| Method | PSNR | SSIM | SAM | PSNR | SSIM | SAM | PSNR | SSIM | SAM |
| Noise | 11.373 | 0.1212 | 47.389 | 11.188 | 0.1137 | 48.025 | 10.839 | 0.1023 | 49.172 |
| TRPCA+BM4D | 38.798 | <u>0.9790</u> | <u>3.7193</u> | 33.657 | <u>0.9342</u> | <u>5.8150</u> | 30.991 | 0.8821 | <u>7.3463</u> |
| SSTV | <u>39.043</u> | 0.9754 | 4.3674 | <u>34.377</u> | 0.9326 | 6.6053 | 31.251 | 0.8734 | 8.8027 |
| LRMR | 35.196 | 0.9488 | 5.6839 | 33.653 | 0.9301 | 6.8313 | <u>31.516</u> | <u>0.8952</u> | 8.6890 |
| LRTR | 36.479 | 0.9629 | 5.1349 | 33.928 | 0.9331 | 6.2357 | 30.968 | 0.8923 | 8.4193 |
| 3DTNN | **41.658** | **0.9920** | **1.8010** | **35.554** | **0.9655** | **3.9101** | **32.398** | **0.9317** | **5.5411** |

## Case 2: fixed Gaussian noise, different impulse noise, and fixed stripe noise.

Table 3: The performance comparison of five competing methods with respect to different impulse noise levels.

| Case | Case 2 | | | | | | | | |
|---|---|---|---|---|---|---|---|---|---|
| Gaussian noise | $\sigma = 0.02$ | | | | | | | | |
| Impulse noise | $\upsilon = 0.1$ | | | $\upsilon = 0.3$ | | | $\upsilon = 0.4$ | | |
| Stripes | added to 10 bands and proportion $p = 10\%$. | | | | | | | | |
| Method | PSNR | SSIM | SAM | PSNR | SSIM | SAM | PSNR | SSIM | SAM |
| Noise | 14.357 | 0.2531 | 41.766 | 9.6182 | 0.0718 | 49.704 | 8.3756 | 0.0470 | 50.771 |
| TRPCA+BM4D | 39.900 | 0.9832 | 3.2894 | 37.273 | 0.9708 | 4.4344 | 33.336 | 0.9240 | 7.0538 |
| SSTV | 40.239 | 0.9804 | 4.0178 | 37.839 | 0.9682 | 4.8038 | 36.336 | 0.9562 | 5.4216 |
| LRMR | 38.597 | 0.9730 | 3.8940 | 32.704 | 0.9189 | 7.4550 | 30.588 | 0.8819 | 9.2499 |
| LRTR | 38.663 | 0.9741 | 3.7062 | 34.617 | 0.9428 | 6.2333 | 31.113 | 0.8717 | 9.2404 |
| 3DTNN | **42.794** | **0.9937** | **1.6046** | **40.345** | **0.9897** | **2.0145** | **38.629** | **0.9856** | **2.3506** |

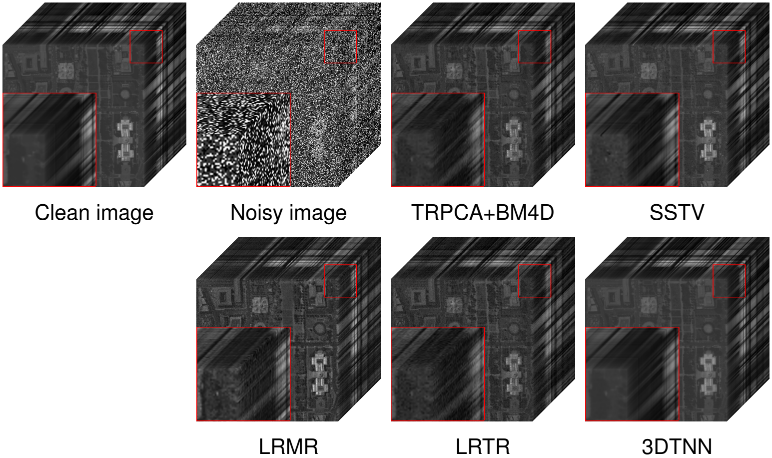


Figure 6: The three dimensional visualization of the denoising results for Gaussian noise with $\sigma = 0.02$ and impulse noise with $\upsilon = 0.4$.

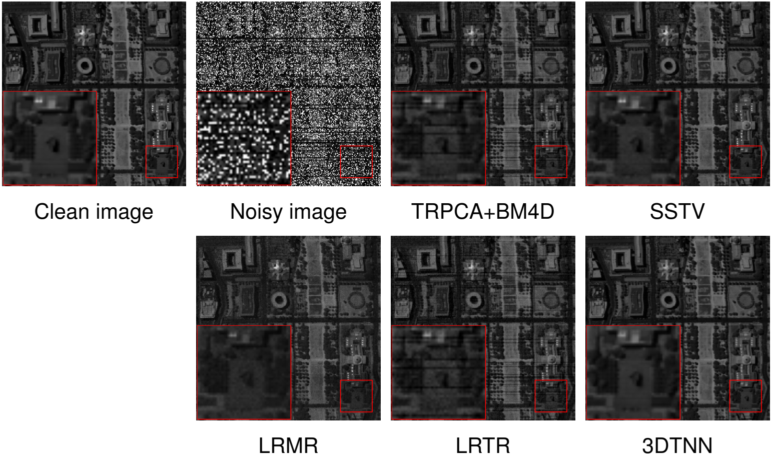


Figure 7: The denoising results at band 131 for Gaussian noise with $\sigma = 0.02$ and impulse noise with $\upsilon = 0.4$.

# Thank you very much for listening.

Wechat

**Homepage: https://yubangzheng.github.io**